SOLA, 2006, Vol. 2, 072–075, doi:10.2151/sola.2006-019

Variation in PSC Occurrence Observed with ILAS-II over the Antarctic in 2003

N. Saitoh[1], S. Hayashida[2], T. Sugita[1], H. Nakajima[1], T. Yokota[1], and Y. Sasano[1]
[1]*National Institute for Environmental Studies, Tsukuba, Japan*
[2]*Faculty of Science, Nara Women's University, Nara, Japan*

Abstract

The Improved Limb Atmospheric Spectrometer (ILAS)-II frequently observed polar stratospheric clouds (PSCs) in the Southern Hemisphere (SH) throughout the winter of 2003. Simultaneous observations of the aerosol extinction coefficient (AEC) at 780 nm, nitric acid, and water vapor data were analyzed to investigate the ambient thermodynamic conditions associated with observed PSCs. PSCs were first observed with ILAS-II at the end of May, and observed most frequently in August/September as temperatures cooled. At approximately 20 km late in the PSC season, however, PSCs were less likely to occur, despite cold temperatures, because of the lower concentration of nitric acid due to denitrification caused by sedimentation of previously occurring PSCs. The probability of PSC occurrence and the probability of ambient temperatures colder than nitric acid trihydrate (NAT) saturation temperature (T_{NAT}) were well correlated below ~20 km throughout the winter. In contrast, PSC frequency at ~22 km from late August to early September was low even when temperatures were sufficiently colder than T_{NAT}; this is, at least, partly because of the decrease in background aerosol particles in the atmosphere.

1. Introduction

Polar stratospheric clouds (PSCs) consist mainly of nitric acid and water/ice and form in winter and early spring in the lower stratosphere over both polar regions (e.g., Solomon 1999). PSCs play a crucial role in ozone depletion processes; they provide surfaces for heterogeneous reactions that convert inactive chlorine into active chorine (e.g., Solomon 1999) and cause denitrification (e.g., Fahey et al. 1990) and nitrification (e.g., Hübler et al. 1990). Activated chlorine causes severe ozone depletion, especially in the Southern Hemisphere (SH), which is known as the "ozone hole". The climatology of PSC frequency in the SH was examined using aerosol data from the Stratospheric Aerosol Measurement (SAM) II from 1978 to 1989 (Poole and Pitts 1994), data from the Polar Ozone and Aerosol Measurement (POAM) II from 1994 to 1996 (Fromm et al. 1997), and data from multiple solar occultation sensors from 1978 to 2000 (Fromm et al. 2003).

Poole and Pitts (1994) examined the relationship between PSC frequency and temperature and showed that PSC formation in the SH is less likely later in PSC season than earlier. Other studies (e.g., Watterson and Tuck 1989; Hervig et al. 1997; Mergenthaler et al. 1997) have suggested that PSC formation late in PSC season in the SH is strongly affected by preceding denitrification and dehydration. However, there have been few studies on the variability of the relationship between PSC frequency and temperature over the course of a PSC season that are based on extensive observations of aerosols, nitric acid, and water vapor in the SH.

Against this background, we used data obtained by the Improved Limb Atmospheric Spectrometer (ILAS)-II over the SH in 2003 to investigate the relationship between PSC occurrence and temperature. ILAS-II is a solar occultation sensor onboard the Advanced Earth Observing Satellite (ADEOS)-II. ILAS-II continuously observed vertical profiles of minor constituent gases and aerosols daily at 14 circumpolar points at high latitudes in each hemisphere (53.9–71.1°N, 63.6–88.0°S) in the stratosphere from April through October 2003 (Nakajima et al. 2006). The ILAS-II Version 1.4 (V1.4) product (Yokota et al. 2006) used in this study contains 2643 profiles for the SH. ILAS-II aerosol extinction coefficient (AEC) data at 780 nm were used to compute the frequency of PSC occurrence. The United Kingdom Meteorological Office (MetO) stratospheric analyses data were used to diagnose the ambient temperature. ILAS-II nitric acid and water vapor data were used to calculate the nitric acid trihydrate (NAT) saturation temperature (hereafter referred to as "T_{NAT}"). T_{NAT} has been widely applied to estimate PSC areal extents (e.g., Rex et al. 1999). This study used T_{NAT} as a reference for the existence of nitric acid-containing particles such as NAT and super-cooled ternary solution (STS). This study therefore considers variations in relationships among PSC frequency, ambient temperature, and T_{NAT} at the ILAS-II measurement locations for the entire SH winter of 2003.

2. PSC identification and T_{NAT} calculation

PSCs were identified from ILAS-II AEC data over the SH using methods similar to those for ILAS data in the NH (Hayashida et al. 2000). First, averages and standard deviations for ILAS-II AEC data at temperatures warmer than 200 K were calculated for each 10-day period and for each altitude level from April to October in 2003. The mean plus five times the standard deviation was defined as a PSC threshold; aerosol data whose extinction exceeded the threshold were then identified as PSCs. This method was applied to all ILAS-II data inside the polar vortex, the boundaries of which were determined using MetO data according to the method by Nash et al. (1996). This approach, however, sometimes could not determine a threshold, mainly in August and September, because all ILAS-II measurement points within a 10-day period had temperatures colder than 200 K. If thresholds could not be determined, then interpolated values were derived from threshold values at the same altitude before and after the period with no threshold.

The ILAS-II V1.4 AEC data at 12–24 km in the SH used in this study were validated by Saitoh et al. (2006). ILAS-II AEC data have a negative bias (12–30% at 20–22 km) relative to the Stratospheric Aerosol and Gas Experiment (SAGE) II Version 6.2 (V6.2) data. However, this negative bias does not affect PSC identification because PSC thresholds adopted here were relative values determined from ILAS-II AEC data themselves.

T_{NAT} values were calculated at all ILAS-II measurement locations inside the polar vortex using the empirical expression by Hanson and Mauersberger (1988). ILAS-II V1.4 nitric acid and water vapor data were used in the calculation. The nitric acid data were validated by Irie et al. (2006), who showed that the precision of the nitric acid data was 13–14, 5, and 1% at 15, 20, and 25 km, respectively. The accuracy was −13/+26% at 15–25 km, which suggests that

Corresponding author and present affiliation: Naoko Saitoh, Center for Climate System Research, University of Tokyo, General Research Building, 5-1-5 Kashiwanoha, Kashiwa-shi, Chiba 277-8568, Japan. E-mail: snaoko@ccsr.u-tokyo.ac.jp.

the nitric acid data are suitable for scientific purposes. The V1.4 water vapor data were compared to coincident Halogen Occultation Experiment (HALOE) water vapor data (Version 19) (Harries et al. 1996) and SAGE II water vapor data (V6.2) (Taha et al. 2004), both of which had been already validated. ILAS-II water vapor data agreed with HALOE and SAGE II data to within 10–15% below 25 km.

The following discussions consider two probabilities: P_{PSC} and $P_{T(NAT)}$. The probability of PSC occurrence (P_{PSC}) and the probability of temperature at the ILAS-II measurement locations colder than T_{NAT} ($P_{T(NAT)}$) were defined as

$$P_{PSC}\ (\%) = \frac{N_{PSC}}{N_{Obs}} \times 100,\ P_{T(NAT)}\ (\%) = \frac{N_{T(NAT)}}{N_{Obs}} \times 100,$$

where N_{Obs} is the number of all ILAS-II measurements, N_{PSC} is the number of data points identified as PSCs, and $N_{T(NAT)}$ is the number of data points colder than T_{NAT}. P_{PSC} and $P_{T(NAT)}$ were calculated for every 10-day period at every altitude level for all the ILAS-II measurement locations inside the polar vortex.

The latitude of ILAS-II measurements shifted poleward from June to September in the range of 23° (65.3–88.0°S; Fig. 1d). Thus, the following time-series data include variability due to seasonal evolution and also due to latitudinal changes.

3. PSC distribution in the SH in 2003

Figure 1a shows daily mean MetO temperatures at ILAS-II measurement locations inside the polar vortex (color shading) and P_{PSC} values computed for each 10-day period from June to October in the SH (hereafter referred to as the "PSC season") (white contour lines). ILAS-II first observed PSCs in the SH at approximately 23 km on 30 May and then continuously observed them until ceasing operation (24 October). PSCs were most frequent (more than ~80% of the time) in August and September. The daily mean MetO temperatures were coldest (colder than ~185 K) in these two months.

At approximately 20 km in September, however, P_{PSC} values were not large despite cold temperatures. Figure 2a shows time-series of daily mean temperature (black) and P_{PSC} (dashed black) at 20 km. P_{PSC} values increased from late July through August, reaching as high as ~80%. However, P_{PSC} dropped to 21% at the end of September, even though temperatures were still as cold as 180–190 K. PSC formation is controlled not only by temperature but also by the partial pressure of nitric acid, and daily mean nitric acid concentrations, represented by color shading in Fig. 1b, were lower in August/September (71.1–88.0°S) than in June/July (65.3~71.1°S). Figure 2a (gray line) shows that the daily mean nitric acid concentration at 20 km in mid-September was 0.7–1.5 ppbv, while the concentration in early July was as high as 5.5–9.3 ppbv. At a given pressure, T_{NAT} is lower for lower nitric acid concentration, so that smaller P_{PSC} can be expected at approximately 20 km in September.

The white contour lines in Fig. 1b show the distribution of $P_{T(NAT)}$. $P_{T(NAT)}$ was well correlated with P_{PSC} below ~20 km. The largest $P_{T(NAT)}$, 80–90%, occurred in late September between 15–17 km and corresponded to the largest P_{PSC}, also 80–90%. Most PSCs were observed at temperatures colder than T_{NAT}. The good correlation between P_{PSC} and $P_{T(NAT)}$ thus suggests that PSCs occurred with high probability if the temperatures were sufficiently colder than T_{NAT}. However, the correlation between $P_{T(NAT)}$ and P_{PSC} was not as strong above ~20 km as below ~20 km. The discrepancy between P_{PSC} and $P_{T(NAT)}$ was significant at ~22 km in late August and early September (area 1). Figure 2(b) shows that $P_{T(NAT)}$ was as high as 89% and 87%, while the corresponding P_{PSC} was as low as 40% and 15% in late August and early September, respectively. The discrepancy in June was not as large, but it reached ~30%. The reason for the discrepancies is discussed in the following section.

Several uncertainties exist in the computations of P_{PSC} and $P_{T(NAT)}$ described above. Appling tolerable ranges for thresholds to identify PSCs did not cause any significant change in P_{PSC}. Irie et al. (2006) showed that ILAS-II nitric acid values are systematically large (14%) at 15–25 km compared to balloon-borne measurements. $P_{T(NAT)}$ values that considered the 14% positive bias differed from the values without the bias by less than 5%. Yokota et al. (2002) and Yokota et al. (2006) suggested that the presence of PSCs yields systematic errors in ILAS-II nitric acid and water vapor data by the nongaseous contribution correction in the retrieval scheme. However, the systematic errors had little effect on $P_{T(NAT)}$ values.

Uncertainties in MetO temperatures directly affect $P_{T(NAT)}$ values. Knudsen et al. (2002) suggested that MetO temperatures have a slight positive bias of ~0.3 K at ~190 K. Here, 0.3 K warm bias was assumed, and $P_{T(NAT)}$ was then recomputed. The recomputed $P_{T(NAT)}$ values were slightly larger, but the characteristics in Fig. 1b remained un-

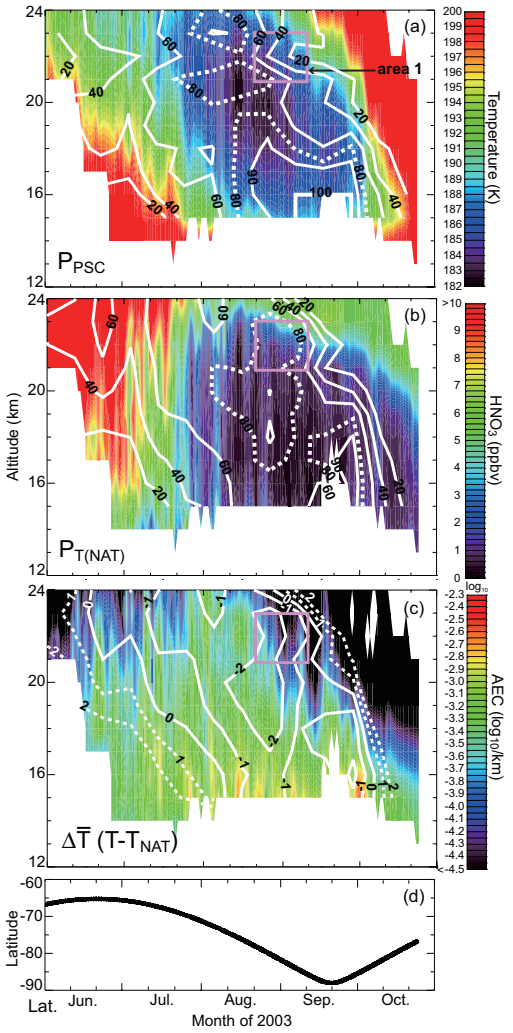

Fig. 1. (a) Time-height cross section of daily mean MetO temperature data at ILAS-II measurement locations (color shading) and P_{PSC} (white contour lines) inside the polar vortex; (b) time-height cross section of daily mean concentrations of ILAS-II nitric acid (color shading) and $P_{T(NAT)}$ (white contour lines) inside the polar vortex; (c) time-height cross section of daily mean values of ILAS-II AEC (color shading) and the difference between ambient MetO temperature and corresponding T_{NAT} ($\Delta\bar{T}$) (white contour lines) inside the polar vortex; (d) latitude of the ILAS-II measurement locations in the SH. For (1)–(3), 80% isopleth lines are dashed. Values of P_{PSC} and $P_{T(NAT)}$ were calculated for each 10-day interval at each altitude level. See text for the definitions.

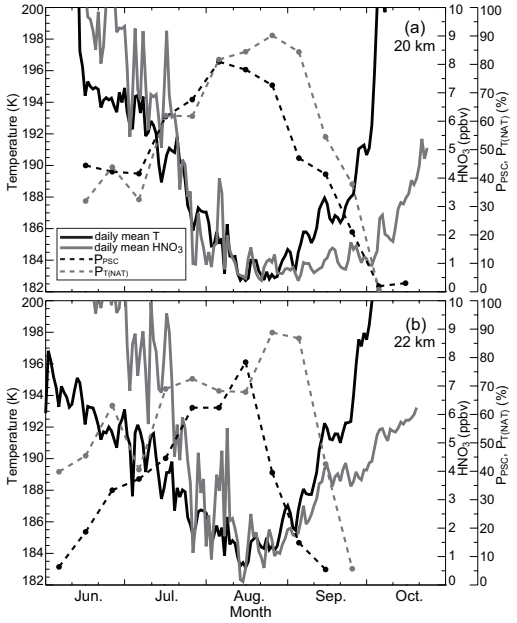

Fig. 2. Time-series of daily mean temperature (solid black line), daily mean nitric acid concentration (solid gray line), P_{PSC} (dashed black line), and $P_{T(NAT)}$ (dashed gray line) inside the polar vortex. Values of P_{PSC} and $P_{T(NAT)}$ depicted by circles were calculated for each 10-day interval at each altitude level; (a) 20 km and (b) 22 km.

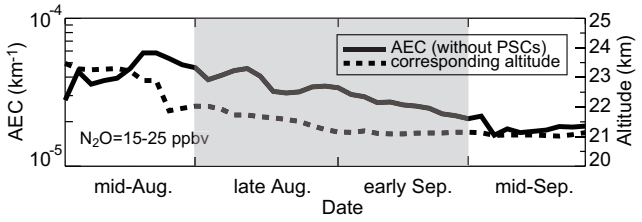

Fig. 3. Time-series of the daily mean ILAS-II AEC (thick black) and corresponding altitude (dashed black) at the iso-N_2O level of 15–25 ppbv inside the polar vortex from mid-August to mid-September. A 10-day running mean was applied. The PSC data identified were excluded from the AEC averages.

changed. The reported temperature bias had little impact on the results presented above.

4. Discussion

Several satellite sensors have observed PSCs in the SH, such as SAM II (Poole and Pitts 1994), POAM II (Fromm et al. 1997), and POAM III (Nedoluha et al. 2003), which had latitudinal coverages similar to the coverage by ILAS-II. All observations, including those by ILAS-II, showed the largest P_{PSC} values in August and September. The P_{PSC} of 40–50% in June 2003 from ILAS-II was large compared to some past measurements; for example, the 10-year ensemble average of P_{PSC} in June between 1978 and 1989 ranged from 5 to 20% (Poole and Pitts. 1994; Fig. 2a) and P_{PSC} values in June from 1994 to 1996 were 15 to 20% (Fromm et al. 1997; Fig. 10), although P_{PSC} in June 2002 was exceptionally high at ~60% (Nedoluha et al. 2003).

The above results show that P_{PSC} was not as large at approximately 20 km in September even though temperatures at the ILAS-II measurement locations were still cold. In other words, PSC formation was less likely late in the PSC season, which is consistent with the results reported by Poole and Pitts (1994). This is due to the low concentration of nitric acid caused by a permanent denitrification in August, as suggested by trajectory analyses coupled with ILAS-II nitric acid and AEC data (Sugita et al. 2005). Our results show that PSC formation at approximately 20 km in the late PSC season is inhibited because of nitric acid depletion attributable to denitrification caused by sedimentation of previous PSCs (e.g., Watterson and Tuck 1989; Mergenthaler et al. 1997).

Most PSCs were observed where temperatures were colder than T_{NAT}. According to the definition of P_{PSC} and $P_{T(NAT)}$, the ratio of P_{PSC} and $P_{T(NAT)}$ ($P_{PSC}/P_{T(NAT)}$) can be expected to be close to the probability of PSC occurrence where temperatures are colder than T_{NAT}. $P_{PSC}/P_{T(NAT)}$ below ~20 km was almost 0.8~0.9, which suggests that PSCs occurred with high probability if the temperatures were colder than T_{NAT}. However, at ~22 km in June, P_{PSC} was not large despite relatively large $P_{T(NAT)}$. This is because the temperature there was only slightly cooler than T_{NAT}. Figure 1c depicts the averaged differences between temperatures at ILAS-II measurement locations inside the polar vortex and the corresponding T_{NAT} as white contour lines of $\Delta\overline{T}$. Temperatures at ~22 km in June were 0–2 K warmer on average than T_{NAT}. It is well-known that STS droplets form at 3–5 K colder than T_{NAT} (e.g., Carslaw et al. 1994), and NAT particles would also form at temperatures several degrees colder than T_{NAT} (Tabazadeh et al. 2001) or at even lower temperatures (Carslaw et al. 1998). Therefore, a high probability of PSC formation (P_{PSC}) cannot be anticipated in June even though $P_{T(NAT)}$ was relatively large.

Discrepancies between P_{PSC} and $P_{T(NAT)}$ were much larger in late August and early September than those in June at the same altitude region. As shown in Fig. 1c, temperatures were more than 1-2 K colder on average than T_{NAT} in late August and early September. A possible explanation for low P_{PSC} values despite such low temperatures is that background aerosol particles that had the potential to nucleate PSCs had already disappeared at these altitude levels. Color shading in Fig. 1c represents daily mean values of ILAS-II AEC; ILAS-II AEC values at ~22 km were much smaller after mid-August than before. This suggests a decrease of background aerosol particles with radii of 0.4–0.5 μm to which ILAS-II extinction measurements are most sensitive.

The decrease in AEC could have been caused both by strong descent motion of upper air with low aerosol concentration inside the polar vortex and "cleansing effect" due to sedimentation of PSCs that had formed previously (e.g., Thomason and Poole 1993). Atmospheric subsidence inside the polar vortex was evident in ILAS-II N_2O and CH_4 data (Ejiri et al. 2006; Fig. 1, 2). To clarify the effect of particle sedimentation, time-series of the AEC at the iso-N_2O level (15 ppbv < N_2O < 25 ppbv) is shown in Fig. 3. The AEC distinctly decreased from mid-August through early-September; this decrease can be attributed to "cleansing" caused by sedimentation of PSCs that occurred earlier in that altitude region. Once "cleansing" occurs, aerosol concentration in the atmosphere cannot increase at high altitudes without aerosol loading from low latitudes coupled with the breakup of the polar vortex (Thomason and Poole 1993). The above results indicate that PSC formation would be inhibited because of a shortage of background aerosol particles in the atmosphere even when ambient temperatures were sufficiently colder than T_{NAT}.

5. Conclusion

ILAS-II frequently observed PSCs from 30 May through October 2003 in the SH. Qualitative agreement was found between cold regions and high P_{PSC} (probability of PSC occurrence) computed from ILAS-II AEC data. Generally, P_{PSC} correlated with low temperatures; P_{PSC} was largest in August/September when temperatures were coldest. However, at approximately 20 km in September, P_{PSC} was not as large even though temperatures were still cold. PSC formation late in the PSC season was less likely due to a

decrease in nitric acid in the atmosphere caused by denitrification. P_{PSC} and $P_{T(NAT)}$ (probability of ambient temperature colder than T_{NAT}) calculated from ILAS-II nitric acid and water vapor data correlated well below ~20 km. PSCs existed in that region with high probability when temperatures were sufficiently colder than T_{NAT}. However, P_{PSC} at ~22 km from late August to early September was small even when $P_{T(NAT)}$ was large, in part because of "clean sing effect" that removed background aerosol particles from the atmosphere. It is suggested that PSC frequency depends on the degree of denitrification and/or the amount of background aerosols that can be nuclei of PSCs. Therefore, T_{NAT} cannot be always a good reference for PSC occurrence, especially above 20 km in late winter.

Acknowledgments

We thank all members of the ILAS-II Science Team and Validation Experiment Team, and their associates. We are grateful to the United Kingdom Meteorological Office (MetO) for supplying the stratospheric analyses data. The ILAS-II data retrieval processing was conducted at the ILAS-II Data Handling Facility (DHF) at the National Institute for Environmental Studies (NIES). The ILAS-II project was funded by the Ministry of the Environment of Japan (MOE). A part of this research was supported by the Global Environment Research Fund provided by the MOE.

References

Carslaw, K. S., B. P. Luo, S. L. Clegg, T. Peter, P. Brimblecombe, and P. J. Crutzen, 1994: Stratospheric aerosol growth and HNO3 gas phase depletion from coupled HNO3 and water uptake by liquid particles, *Geophys. Res. Lett.*, **21**, 2479–2482.

Carslaw, K. S., M. Wirth, A. Tsias, B. P. Luo, A. Dornbrack, M. Leutbecher, H. Volkert, W. Renger, J. T. Bacmeister, and T. Peter, 1998: Particle microphysics and chemistry in remotely observed mountain polar stratospheric clouds, *J. Geophys. Res.*, **103**, 5785–5796.

Ejiri, M. K., Y. Terao, T. Sugita, H. Nakajima, T. Yokota, G. C. Toon, B. Sen, G. Wetzel, H. Oelhaf, J. Urban, D. Murtagh, H. Irie, N. Saitoh, T. Tanaka, H. Kanzawa, M. Shiotani, H. Kobayashi, and Y. Sasano, 2006: Validation of the Improved Limb Atmospheric Spectrometer-II (ILAS-II) Version 1.4 Nitrous Oxide and Methane profiles, *J. Geophys. Res.*, in revision.

Fahey, D. W., S. Solomon, S. R. Kawa, M. Loewenstein, J. R. Podolske, S. E. Strahan, and K. R. Chan, 1990: A diagnostic for denitrification in the winter polar stratospheres, *Nature*, **345**, 698–702.

Fromm, M. D., J. D. Lumpe, R. M. Bevilacqua, E. P. Shettle, J. Hornstein, S. T. Massie, and K. H. Fricke, 1997: Observations of Antarctic polar stratospheric clouds by POAM II: 1994-1996, *J. Geophys. Res.*, **102**, 23659–23672.

Fromm, M., J. Alfred, and M. Pitts, 2003: A unified, long-term, high-latitude stratospheric aerosol and cloud database using SAM II, SAGE II, and POAM II/III data: Algorithm description, database definition, and climatology, *J. Geophys. Res.*, **108**, doi:10.1029/2002JD002772.

Hanson, D., and K. Mauersberger, 1988: Laboratory studies of the nitric acid trihydrate: Implications for the south polar stratosphere, *Geophys. Res. Lett.*, **15**, 855–858.

Harries, J. F., J. M. R. III, A. F. Tuck, L. L. Gordley, P. Purcell, K. Stone, R. M. Bevilacqua, M. Gunson, G. Nedoluha, and W. A. Traub, 1996: Validation of measurements of water vapor from the Halogen Occultation Experiment (HALOE), *J. Geophys. Res.*, **101**, 10205–10216.

Hayashida, S., N. Saitoh, A. Kagawa, T. Yokota, M. Suzuki, H. Nakajima, and Y. Sasano, 2000: Arctic polar stratospheric clouds observed with the Improved Limb Atmospheric Spectrometer during winter 1996/1997, *J. Geophys. Res.*, **105**, 24715–24730.

Hervig, M. E., K. S. Carslaw, T. Peter, T. Deshler, L. L. Gordley, G. Redaelli, U. Biermann, and J. M. R. III, 1997: Polar stratospheric clouds due to vapor enhancement: HALOE observations of the Antarcitc vortex in 1993, *J. Geophys. Res.*, **102**, 28185–28193.

Hübler, G., D. W. Fahey, K. K. Kelly, D. D. Montzka, M. A. Carroll, A. F. Tuck, L. E. Heidt, W. H. Pollock, G. L. Gregory, and J. F. Vedder, 1990: Redistribution of reactive odd nitrogen in the lower Arctic stratosphere, *Geophys. Res. Lett.*, **17**, 453–456.

Irie, H., T. Sugita, H. Nakajima, T. Yokota, H. Oelhalf, G. Wetzel, G. C. Toon, B. Sen, M. L. Santee, Y. Terao, N. Saitoh, M. K. Ejiri, T. Tanaka, Y. Kondo, H. Kanzawa, H. Kobayashi, and Y. Sasano, 2006: Validation of stratospheric nitric acid concentration profiles observed by ILAS-II, *J. Geophys. Res.*, **111**, doi: 10.1029/2005JD006115.

Knudsen, B. M., J.-P. Pommereau, A. Garnier, M. Nunes-Pinharanda, L. Denis, P. Newman, G. Letrenne, and M. Durand, 2002: Accuracy of analyzed stratospheric temperatures in the wineter Arctic vortex from infrared Montgolfier long-duration balloon flights 2. Results, *J. Geophys. Res.*, **107**, doi:10.1029/2001JD001329.

Mergenthaler, J. L., J. B. Kumer, A. E. Roche, and S. T. Massie, 1997: Distribution of Antarctic polar stratospheric clouds as seen by the CLAES experiment, *J. Geophys. Res.*, **102**, 19161–19170.

Nakajima, H., T. Sugita, T. Yokota, H. Kobayashi, Y. Sasano, T. Ishigaki, Y. Mogi, N. Araki, K. Waragai, N. Kimura, T. Iwasawa, A. Kuze, J. Tanii, T. Togami, H. Kawasaki, M. Horikawa, and N. Uemura, 2006: Characteristics and performance of the Improved Limb Atmospheric Spectrometer-II (ILAS-II) onboard the ADEOS-II satellite, *J. Geophys. Res.*, in press.

Nash, E. R., P. A. Newman, J. E. Rosenfield, and M. R. Schoeberl, 1996: An objective determination of the polar vortex using Ertel's potential vorticity, *J. Geophys. Res.*, **101**, 9471–9478.

Nedoluha, G. E., R. M. Bevilacqua, M. D. Fromm, K. W. Hoppel, and D. R. Allen, 2003: POAM measurements of PSCs and water vapor in the 2002 Antarctic vortex, *Geophys. Res. Lett.*, **30**, doi:10.1029/2003GL017577.

Poole, L. R., and M. C. Pitts, 1994: Polar stratospheric cloud climatology based on Stratospheric Aerosol Measurement II observations from 1978 to 1989, *J. Geophys. Res.*, **99**, 13083–13089.

Rex, M., et al., 1999: Chemical ozone loss in the Arctic winter 1994/95 as determined by the MATCH technique, *J. Atmos. Chem.*, **32**, 35–59.

Saitoh, N., S. Hayashida, T. Sugita, H. Nakajima, T. Yokota, M. Hayashi, K. Shiraishi, H. Kanzawa, M. K. Ejiri, H. Irie, T. Tanaka, Y. Terao, R. M. Bevilacqua, C. E. Randall, L. W. Thomason, G. Taha, H. Kobayashi, and Y. Sasano, 2006: Intercomparison of ILAS-II Version 1.4 aerosol extinction at 780 nm with SAGE II, SAGE III, and POAM III, *J. Geophys. Res.*, in press.

Sasano, Y., T. Yokota, H. Nakajima, T. Sugita, and H. Kanzawa, 2000: ILAS-II instrument and data processing system for stratospheric ozone layer monitoring, *Proc. SPIE*, pp. 106–114, Sendai, Japan.

Solomon, S., 1999: Stratospheric ozone depletion: A review of concepts and history, *Rev. Geophys.*, **37**, 275–316.

Sugita, T., N. Saitoh, H. Nakajima, T. Yokota, T. Imamura, and Y. Sasano, 2005: Short time variations in HNO3 and aerosol extinction coefficient data as observed by ILAS-II in the 2003 Antarctic stratosphere, *Solar Occultation Satellite Science Team Workshop*, Maryland, USA.

Tabazadeh, A., E. J. Jensen, O. B. Toon, K. Drdla, and M. R. Schoeberl, 2001: Pole of the stratosphere polar freezing belt in denitrification, *Science*, **291**, 2591–2594.

Taha, G., L. W. Thomason, and S. P. Burton, 2004: Comparison of Stratospheric Aerosol and Gas Experiment (SAGE) II version 6.2 water vapor with balloon-borne and space-based instruments, *J. Geophys. Res.*, **109**, doi:10.1029/2004JD004859.

Thomason, L. W., and L. R. Poole, 1993: Use of stratospheric aerosol properties as diagnostics of Antarctic vortex processes, *J. Geophys. Res.*, **98**, 23003–23012.

Watterson, I. G., and A. F. Tuck, 1989: A comparison of the longitudinal distributions of polar stratospheric clouds and temperature for the 1987 Antarctic spring, *J. Geophys. Res.*, **94**, 16511–16525.

Yokota, T., H. Nakajima, T. Sugita, H. Tsubaki, Y. Itou, M. Kaji, M. Suzuki, H. Kanzawa, J. H. Park, and Y. Sasano, 2002: Improved Limb Atmospheric Spectrometer (ILAS) data retrieval algorithm for Version 5.20 gas profile products, *J. Geophys. Res.*, **107**, doi:10.1029/2001JD000628.

Yokota, T., H. Nakajima, T. Sugita, S. Oschepkov, M. Horikawa, M. Usami, H. Kawasaki, N. Uemura, Y. Itou, M. Kaji, H. Kobayashi, and Y. Sasano, 2006: Improved Limb Atmospheric Spectrometer-II (ILAS-II) Version 1.4 algorithm for retrieval of gas and aerosol profiles in the stratosphere, in preparation.

Manuscript received 11 November 2005, accepted 17 April 2006
SOLA: http://www.jstage.jst.go.jp/browse/sola/